Rock Mechanics in the National Interest, Elsworth, Tinucci & Heasley (eds),
© 2001 Swets & Zeitlinger Lisse, ISBN 90 2651 827 7

Numerical geomechanical modeling for Stillwater Mine, Nye, Montana

M.M.MacLaughlin
Montana Tech of The University of Montana, Butte, Montana, USA

R.B.Langston
Stillwater Mining Company, Nye, Montana, USA

T.M.Brady
National Institute for Occupational Safety and Health – Spokane Research Laboratory, Spokane, Washington, USA

ABSTRACT: A geomechanical numerical modeling research project is being conducted for the Stillwater Mine located in Nye, Montana. The project involves identifying potential ground control problems and exploring various methods of modeling the behavior of the rock, with objectives of improving underground safety and facilitating optimum support design. During the preliminary modeling stage of the project, it was determined using continuum-based approaches that the discontinuities can control the behavior of the rock; the data collection system at the mine was subsequently adjusted to provide more information about the rock joints. A parametric study of possible underground conditions at one specific site was then conducted using discrete element methods. The results compare well with a rough analysis of the conditions. A discussion of the strengths and limitations of the methods employed and the significance of the results is included.

1 INTRODUCTION

A geomechanical numerical modeling research project is being conducted at the Stillwater Mine, a large underground platinum/palladium mine located in Nye, Montana. The project involves identifying potential ground control problems and exploring various methods to model the behavior of the rock. The primary objectives are to improve safety for miners working underground, and to develop a modeling system that will facilitate optimum support design. The work presented here contains selected results of the preliminary stage of the project; this paper is not meant to serve as an in-depth case study but rather as an example of the application of a general methodology which can be used to identify the need for discrete element modeling.

The Stillwater Mine has been in operation for 15 years. At the current time, development consists of more than 5 miles of underground excavations, and annual production is approximately 650,000 tons of ore (anonymous, 2001).

The first stage of the numerical modeling project, the preliminary modeling stage, consisted of two parts. First, numerical models based on continuum approaches, finite element and finite difference methods, were used to calculate the stresses and deformations in the rock mass, and determine the overall response to the planned excavations at one specific site within the mine. The results indicated that the discontinuities can in fact control the behavior of the rock, and are a crucial component of the numerical model. The data collection system at the mine has subsequently been adjusted to provide more information regarding the orientation and spacing of the rock joints.

The second part of the preliminary modeling stage involved developing a geomechanical numerical model using discrete element methods to characterize the behavior of the rock. Discrete element methods were developed specifically to model the behavior of discontinuous materials like jointed rock masses and therefore provide more accurate results than continuum-based methods. In this preliminary discontinuum phase, a parametric study of possible underground conditions at the specific site was conducted to examine the potential range of responses. These predictions will later be compared to the actual rock mass behavior.

The site conditions and the details and results of the preliminary modeling stage of the research project are presented in the following sections. This is followed by a comparison of the results with a rough analytical solution, and a discussion of the strengths and limitations of the numerical methods employed.

Many numerical modeling parametric studies have previously been conducted for mining-related applications. Examples include Hart et al 1988, Al-Harthi & Hencher 1992, Coulthard et al 1992, Eve 1996, Trueman et al 1996, and Jung et al 1999. Shen & Barton (1997) used UDEC to investigate circular openings. Grenon et al (2000) conducted a discrete element study very similar to the one described here.

2 SITE CONDITIONS

The Stillwater Mine is situated in an intrusive igneous formation known as the Stillwater Complex. The tabular-shaped layered mafic intrusion was originally sub-horizontal, but has been tilted upward due to subsequent tectonic activity. The platinum and palladium ore-bearing zone now strikes 290° and dips 45° to 70° to the north, and typically ranges from 1 to 2m in thickness (Czamanske & Zientek 1985). The dominant discontinuity orientation is parallel or sub-parallel to this orientation, with additional discontinuities in other orientations.

As documented in several unpublished reports (Kirsten 1997, Langston 1997, Johnson et al 1997, Kirsten & Langston 1998), the plagioclase and olivine-rich coarsely crystalline rocks are of fair quality (Q-values typically ranging from 0.5 to 5). The hanging wall material is slightly less competent than the footwall and ore zone rock, but similar enough to be modeled with the same properties. The intact rock itself is quite strong (unconfined compressive strength 100-120 MPa, friction angle 35° and cohesion 2-12 MPa) and stiff (Young's modulus 120 GPa, Poisson's ratio 0.3). However, the blocky nature of the material tends to produce structurally controlled modes of failure. Alteration of the olivine to serpentine and chlorite along joint surfaces has reduced their shear strength to as low as friction angles of 10°-15°, and this is further exacerbated by the existence of zones of weakness in the hanging wall.

One set of *in situ* stress measurements is available for the site (Langston 1997, Johnson et al 1999). The measurements were made at the eastern end of the footwall drift on the 3200 level of the mine. The major principal stress is approximately 24 MPa, dipping slightly to the north, perpendicular to the strike of the ore zone. The intermediate stress is 18MPa, subhorizontal, parallel to the ore zone. The minimum stress is 12 MPa, subvertical. These measurements agree very well with evidence of stress orientations inferred from the geological features of the site. Although the specific site modeled was located approximately 180m above and some 100m horizontally offset from the site of these measurements, it was decided that the observed stress values would be appropriate to use, and the numerical models were constructed using a horizontal major principal stress of 24 MPa, a vertical minor principal stress of 12 MPa, and an out-of-plane stress of 18 MPa.

The two types of stope designs used for ore production at the mine are long-hole back stopes that are mined from one lower drift, and sub-level stopes that are drilled from a top drift and mucked from below. Support designs typically consist of rockbolt patterns supplemented with cable bolts when less than ideal ground conditions dictate.

The specific site chosen for this study is the 38E200 sublevel stope. The design consisted of excavating the 9m wide by 3m high upper drift first, then a slightly wider 12m by 3m drift, located 7.5m below and 6m to the north.

3 CONTINUUM-BASED MODELS

The first part of the preliminary stage of the numerical modeling project involved continuum-based analysis of the rock mass. The objectives were to calculate the stresses and deformations in the rock mass induced by the planned excavations, and predict the overall response.

Two different numerical modeling methods were used and compared: a finite difference program called FLAC (Itasca 1998) and a finite element program called Phase^2 (Rocscience 1999). Although there are subtle but important internal differences between these two methods, they perform the same basic type of analysis. Both methods involve discretization of the area to be investigated into small connected elements or zones. Figure 1 shows the discretized FLAC "grid" and the Phase^2 "mesh." Although they are not identical, there are more than 10,000 zones or elements in each model. Figure 2 shows a magnified view of the area near the excavations. Note that one of the slight differences is that the sides of the drift are inclined parallel to the ore zone boundaries in the FLAC grid, and vertical in the Phase^2 mesh. The models were constructed in this manner for convenience, and the difference did not affect the results.

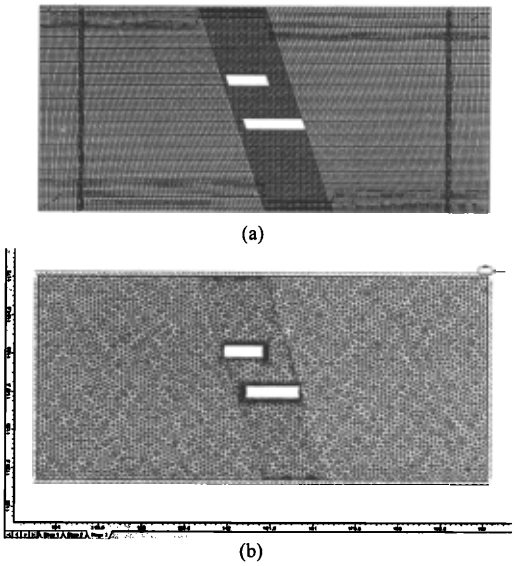

(a)

(b)

Figure 1. Discretization of the geometry of the 38E200 site. (a) finite difference (FLAC) grid. (b) finite element (Phase^2) mesh.

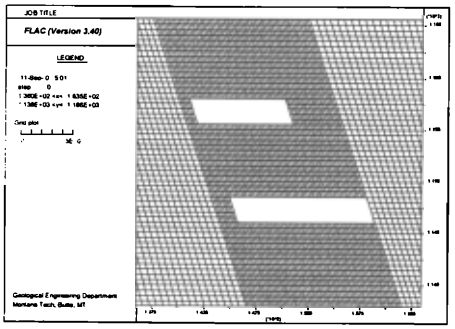

(a)

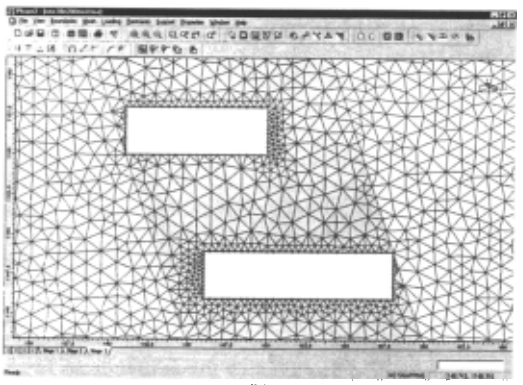

(b)

Figure 2. A close-up view of the area immediately surrounding the excavations. (a) finite difference (FLAC) grid. (b) finite element (Phase^2) mesh.

These programs were used to model the site first as a completely continuous rock mass, with a staged excavation sequence in which the top drift was excavated first, followed by the lower drift. The FLAC and Phase^2 results following excavation of the top drift are shown in Figures 3a and 3b. Figure 4 shows the results after both drifts have been excavated. Both figures show contours of factor of safety as defined by the Mohr-Coulomb failure criterion. Unsurprisingly, the results are very similar: there are areas of low factor of safety immediately above and below the openings, and high factor of safety on either side. The two drifts are close enough to influence each other, but the strength of the rock is high enough to prevent shear failure. Note that the results produced are nearly identical even though the FLAC analyses were performed with stress boundary conditions and the Phase^2 analyses used fixed (zero) displacement boundary conditions.

In order to account for potential fractures in the rock, the analysis was repeated using the ubiquitous joint material model. This model accounts for anisotropic strength resulting from planes of

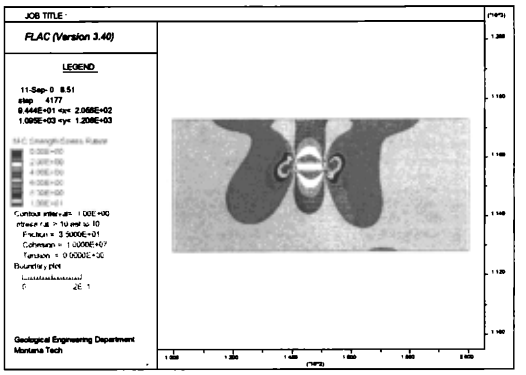

(a)

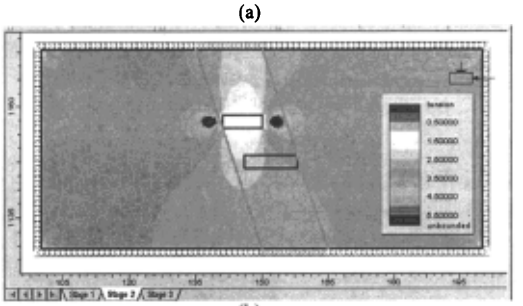

(b)

Figure 3. Contours of factor of safety following excavation of the top drift. (a) finite difference (FLAC) model. (b) finite element (Phase^2) model.

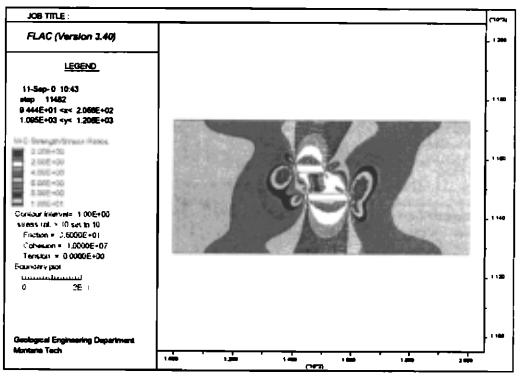

(a)

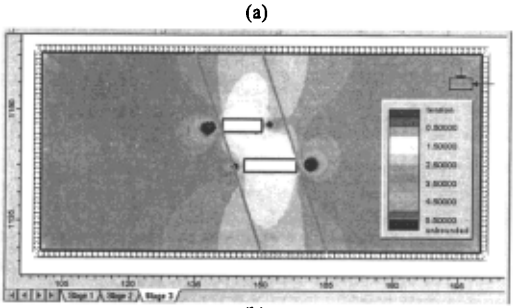

(b)

Figure 4. Contours of factor of safety following excavation of both drifts. (a) FLAC model. (b) Phase^2 model.

weakness caused by an infinite number of closely spaced parallel joints. While it is theoretically possible to model several sets of joints using this method, a rock mass would realistically only have one set of these joints. For this project it was assumed that there is a set of ubiquitous joints parallel to the ore zone boundaries, with friction angle = 15° and cohesion = 0. The results of the Phase^2 analysis are shown in Figure 5. The contours of factor of safety are shown after excavation of the top drift (a) and both drifts (b). Note that there is a small area immediately above and below the top drift with factor of safety less than 1.0, indicating potential shear failure of the rock, and after excavation of the lower drift, that region greatly expands and extends between the two openings. The FLAC analysis showed that the system was unable to reach equilibrium, indicating that the material was failing. Again, the two methods are in agreement.

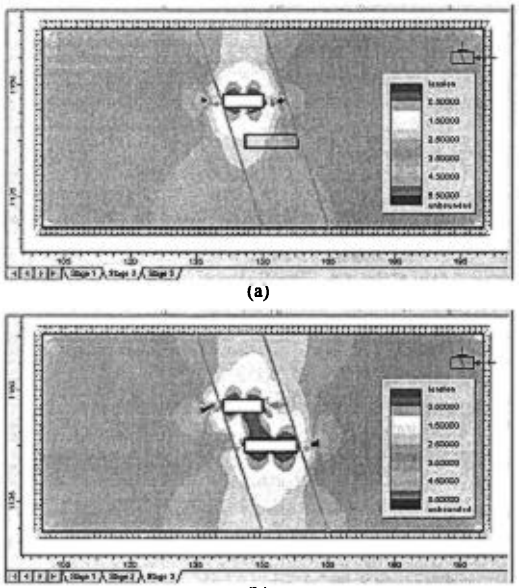

(a)

(b)

Figure 5. Contours of factor of safety with ubiquitous joints parallel to the ore zone boundaries, as determined by the finite element (Phase^2) analysis, (a) following excavation of the top drift, and (b) following excavation of both drifts.

To further quantify the effects of the ubiquitous joints, several additional aspects were investigated in detail. First, the orientation of the ubiquitous joints was varied to determine if equilibrium could be reached with joints that were not parallel to the ore zone boundaries. Failure occurred in all orientations, and in fact is much more pronounced as the ubiquitous joint orientation approaches horizontal, parallel to the major principal stress. Second, the shear strength of the ubiquitous joints (again oriented parallel to the ore zone boundaries) was increased in an attempt to reach equilibrium; even with unrealistically high values (friction angle = 85° and cohesion = 5000 GPa) the models predicted failure of the material.

The results of the continuum-based analyses indicate that the excavations will be safe if there are no joints in the rock, but that failure will occur if an infinite number of joints exist. Representing the rock mass as perfectly continuous is unconservative – it may overestimate the factor of safety. However, using the ubiquitous joint material model, and thereby drastically reducing the rock strength in the plane of the joints, is extremely overconservative. Another interpretation of the results is that the presence of discontinuities in the rock mass can reduce the strength enough to cause shear failure. The real rock mass will have a particular number of joints, a situation somewhere in between the conditions investigated with the continuum methods. The question whether that particular number of joints is sufficient to cause failure cannot easily be answered using the results of the continuum-based analyses. Creating a model with a significant but finite number of joints, in order to more adequately represent the field conditions, is possible with these continuum-based methods but not very practical. More appropriate tools are available to model fractured rock, as discussed in the following section.

As an alternative to explicitly modeling the presence of particular discontinuities, it is possible to represent the jointed rock as a "continuous" material with lower strength than the intact rock. This may be conveniently accomplished via the Hoek-Brown failure criterion, which uses the unconfined compressive strength of the rock and two additional parameters (m, a function of the rock type, and s, degree of fracturing) to characterize the behavior. Although this is a valid approach and has produced some interesting results, they will not be discussed in this paper due to space limitations.

The most significant results of the continuum modeling phase are that the conditions at the site indicate that the presence of joints and fractures in the rock can control the stability of the excavations, and that more detailed analysis using discontinuum-based techniques is warranted. In order to use these tools effectively, more specific information is required regarding the fractures in the rock mass. Based on the evidence from the preliminary continuum-based analyses done in this study indicating that the discontinuities can control the behavior of the rock mass, the geomechanics data collection system at the Stillwater Mine was subsequently adjusted to facilitate collection of the required discontinuity information. Previously,

observations concerning the size of the blocks and the strength of the fractures were collected, in addition to information about the overall behavior of the rock mass. Data describing the orientation, spacing, and persistence for all of the significant joint sets are also recorded in the current system.

4 DISCONTINUUM-BASED MODELS

Because of the limitations of the continuum-based methods, a different approach was used in the next part of the study: discontinuum modeling. A number methods have been developed specifically to model the behavior of fractured rock masses. The primary difference between discontinuum models, such as the discrete element methods, and the continuum models (finite element and finite difference methods), is that the material is composed of individual blocks that are allowed to move in a completely discontinuous fashion. They are not constrained to remain attached to their original neighbors. In order to allow this to happen, discrete element methods must account for identifying contact between blocks because the contacts may change as the analysis progresses.

Two different discrete element methods will be used in the discontinuous analysis part of this study: the distinct element method as implemented in the UDEC software (Itasca 2000), and discontinuous deformation analysis via the DDA software (Shi 1993). There are subtle but significant differences between these two methods related to the formulation and solution of the equilibrium equations as well as the numerical contact routines. However, they are expected to produce similar results. At the current time, only the UDEC results have been generated, so it is not possible to discuss the comparison.

In addition to general information regarding rock properties and *in situ* stresses, described previously in Section 2, the discrete element methods require detailed information about the joints and other discontinuities. Since specific rock mass data was not available prior to excavation of the drifts, it was necessary to estimate the possible range of conditions at the site, in order to conduct a parametric study of the rock mass behavior. It was assumed that one primary joint set exists with an orientation parallel to the ore zone boundaries (Joint Set #1), dipping 70° to the North (right side of the page) with variable spacing and friction angle. The parameters studied were a) the dip angle of an assumed second joint set (Joint Set #2) crossing Joint Set #1, b) the friction angle of the joints (assuming Joint Sets #1 and #2 have the same friction angle, and neither joint set has cohesion), and c) the spacing of the joints (Joint Sets #1 and #2 were assumed to have different spacings).

Joint Set #2 was specified to dip to the South (left) - in the opposite direction as Joint Set #1, with angles of 15°, 30°, 45°, 60°, and 75°. Examples of the 30° and 45° cases are shown in Figure 6. The friction angles used for the joints were 15°, 30° and 45°. The joint spacings used were constructed to produce equidimensional blocks in the footwall and ore zone, and tabular blocks with an aspect ratio of approximately 4:1 in the hanging wall. Three categories of spacings were chosen for the footwall and ore zone: 2m, 0.5m, and 0.15m; and three more for the hanging wall: 6m x 1.5m, 2m x 0.5m, and 0.6m x 0.15m. This produced large, intermediate, or small blocks in each region and created 9 possible combinations of block sizes for the analyses. Even with this limited number of possibilities to investigate, a complete suite of analyses consisted of (9 possible block size combinations) x (5 joint dip angle possibilities) x (3 friction angle choices) = a total of 135 unique cases. The 135 cases were then further compounded with investigation of boundary conditions (fixed vs stress, different distances from the opening), rigid vs deformable blocks, joint normal and shear stiffness values, and specifying the locations of specific joints to produce the largest possible unstable system of blocks.

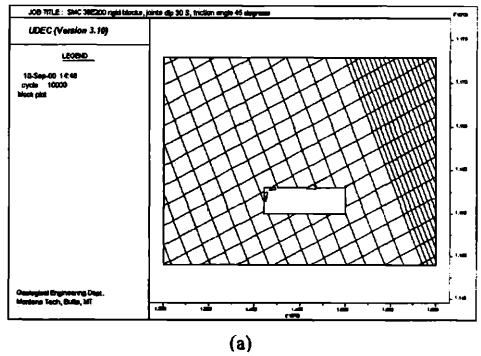

(a)

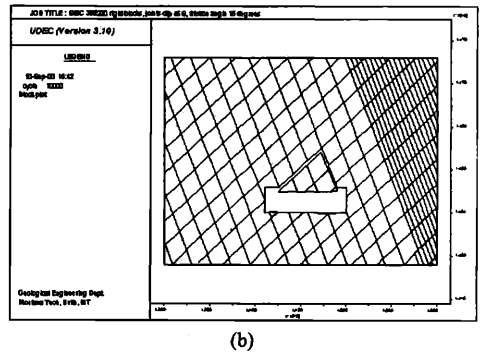

(b)

Figure 6. The geometry of the 38E200 top drift, as modeled with UDEC, with large blocks in the footwall and ore zone, and intermediate blocks in the hanging wall. Joint Set #1 dips to the North (right) at 70°, Joint Set #2 dips to the South (left) with angles of (a) 30°, (b) 45°.

Note that due to the large computation time associated with configurations with many blocks, the first analyses were performed on top drift alone. To date, the bottom drift, which has a wider span that passes closer to the hanging wall, has not been investigated, nor has the configuration with both excavations. Preliminary analyses were first performed on a very limited region surrounding the top drift (shown in Figures 6 and 7), primarily the space above the drift since the block movements were gravity-induced and hardly any movement occurred below or to the sides of the excavation. While these and many discrete element models, for example Grenon et al (2000), were constructed using the rule of thumb that generally acceptable "boundary sizes" are approximately five "object sizes" (Itasca 2000) this approach is not necessarily valid for situations in which the excavation size increases greatly during the analysis as blocks fall and detach themselves from the main rock mass. Preliminary models can be used to determine the approximate final "object size," with subsequent model boundary locations adjusted to account for enlargement of the excavation. Note that the enlargement often occurs in a particular direction instead of uniformly around the opening, so the excavation should not necessarily be centered in the modeling region.

UDEC is capable of modeling the behavior of both deformable blocks and rigid ones. Although both types of analyses were performed in this study, most of the examples presented here contain rigid blocks. The deformable block results did not appear to be significantly different for the conditions investigated in this study, with the primary exception being noticeably larger upward displacements of blocks in the floor of the excavation. Although the analyses with the deformable blocks take much more time due to the computational effort involved, UDEC does provide a greater number of output features for deformable block analyses.

The preliminary limited-region section of the discontinuous analysis part of the study produced a number of interesting results. First, it was determined that the intermediate sized blocks in the footwall and ore zone area were small enough relative to the size of the opening (spacing less than 6% of the span) that the deformation pattern was essentially that of a "continuous" particulate material, appropriately modeled with continuum-based methods. Grenon et al (2000) also documented this behavior with blocks smaller than 5% of the span of the opening. (Shen & Barton (1997) recorded consistent blocky behavior with spacings smaller than 6% of the opening diameter, but their analyses were conducted using round openings.) Since it is logical to assume that the smallest blocks (2% of the span) would behave in a similar or even more pronounced continuous fashion, the most computationally intensive analyses involving the cases with the smallest block sizes were not attempted. Although further investigation of the influence of the joint spacing is being conducted, the results presented here are limited to the cases with large blocks (spacing 22% of the span) in the footwall and ore zone, and intermediate-sized blocks in the hanging wall.

During the limited-region analyses performed with this particular combination of block sizes, three basic types of behavior were found: (a) very little instability or none at all as shown in Figure 6a, (b) instability in a triangular-shaped roof wedge whose size is controlled by the excavation span and intersection angle between Joint Sets #1 and #2, as shown in Figure 6b, and (c) potential deep-seated instability of the roof, shown in Figure 7. While type (a) behavior is obviously safe, and type (b) behavior is almost certainly controlled with adequate support, type (c) behavior may well pose a threat to the safety of the mine workers.

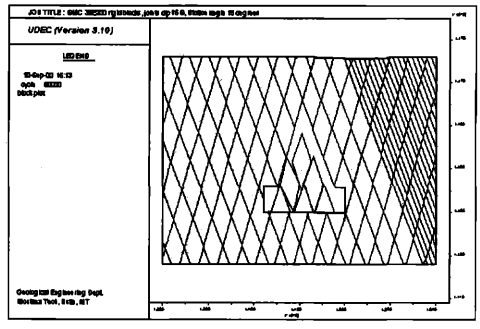

(a)

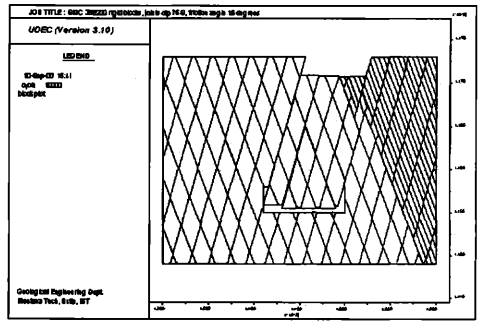

(b)

Figure 7. Deep-seated mode of failure observed in the case with Joint Set #2 dipping 75° S and friction angle of 15°. (a) With 6.3m wedge base width, material above wedge moved slowly and stabilized. (b) With 8.0m wedge base width, whole roof failed catastrophically.

Although only two of the cases analyzed, the combination of the steepest dip angles for Joint Set

#2 (60° and 75°) and the lowest joint friction angle (15°), resulted in potential deep-seated instability, this particular case is significant because very small changes in the geometry parameters produced drastically different behavior. The deep-seated instability (above the unstable roof wedge) with joints dipping 75° as shown in Figure 7a manifested itself as slow movements that eventually stabilized, as did the configuration with joints dipping 60°. The geometry in Figure 7b, identical to 7a but with joint locations specified near the corners of the excavation to maximize the size of the unstable wedge and resulting in a 25% wider base, failed catastrophically. Furthermore, increasing the friction angle just a few degrees results in a much more stable situation. A sharp change in behavior was found for the configuration in Figure 7b between friction angles of 17° (unstable) and 18° (stable). While this type of phenomenon is well recognized in the field of rock mechanics (Amadei 2000), it demonstrates the importance of performing a thorough, comprehensive suite of analyses with a range of input data that is as wide as possible.

These limited-region analyses were used in an extensive but somewhat superficial parametric study that facilitated identification of different types of possible behavior. Although they served their purpose, the results were most likely influenced by boundary effects. The case with Joint Set #2 dipping 75° with maximized wedge size was particularly suspect due to the close proximity of the wedge apex to the boundary of the model. A second more detailed suite of analyses was then performed in which the most critical types of behavior were studied more completely using a much larger region around the excavation, extending to 4.5 drift-widths to either side, 10 drift-heights below, and 13 drift-heights above. The less critical conditions were also double-checked for reassurance, and the range of dip angles for Joint Set #2 was expanded to include vertical joints as well as dip angles of 15°, 30°, 45°, 60°, and 75° to the North, now encompassing the full possible spectrum in 15° increments. Several examples of analyses are shown in Figure 8. The results of the analyses are summarized in Table 1. In general, the stability increased with increasing friction angle, as expected. The stability also increased with increasing dip angle, which produced wedges whose sides are more perpendicular to the horizontal orientation of the major principle stress.

Two of the key questions that were investigated in this part of the study are: Is the catastrophic failure of the 75° maximized wedge solely due to boundary influences? If so, is the potential deep-seated instability mode real or boundary-controlled? The results show that catastrophic movement is indeed an artifact of the limited-region model boundaries being located too close to the failing wedge. However, the deep-seated but less catastrophic mode of failure is possible with friction angles less than 13°, as shown in Figure 9.

Table 1. Behavior displayed by the rock mass, as a function of the dip angle of Joint Set #2, and friction angle of the joints.

Dip of Joint set #2	Friction angle of joints 15°	30°	45°
15° S	roof wedge unstable	roof wedge unstable	roof wedge unstable
30° S	roof wedge unstable	roof wedge unstable	minor instability
45° S	roof wedge unstable	roof wedge unstable	minor instability
60° S	roof wedge unstable	roof stable	roof stable
75° S	roof wedge unstable	roof stable	roof stable
90°	roof stable	roof stable	roof stable
75° N	roof stable	roof stable	roof stable
60° N	roof stable	roof stable	roof stable
45° N	roof stable	roof stable	roof stable
30° N	roof wedge unstable	roof stable	roof stable
15° N	roof wedge unstable	minor instability	minor instability

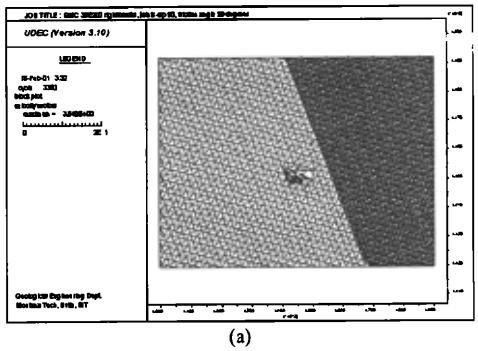

(a)

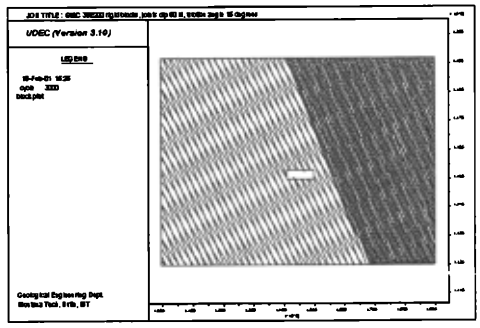

(b)

Figure 8. Models with expanded area. Joint Set #2 dips to the North (right) with angles of (a) 15°, and (b) 60°. Friction angle in both cases is 15°.

Detailed quantification of the size of unstable area is an important item to consider in this type of analysis. A number of measures of instability may be used to evaluate the results. In the rigid block

analyses conducted for this study, a combination of block configuration (Figure 9) and displacement vector plots (Figure 8a) and time histories of the y-component of the velocity vectors (Figure 10) were used. Grenon et al (2000) used a more sophisticated approach: identification of all blocks whose contact stress values were less than 10% of the *in situ* stresses. Analyses using deformable blocks may be evaluated using filled-contour plots of displacement or velocity vector components, principle stress overlays, and plasticity plots. Shen & Barton (1997) made extensive use of open and shear contact state distribution plots.

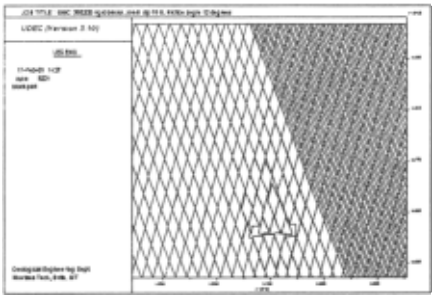

Figure 9. Deep-seated failure mode observed in the case with Joint Set #2 dipping 75° to the South with friction angle of 12°. (Close-up of region around excavation.)

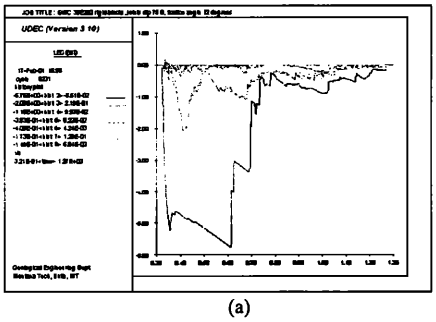

(a)

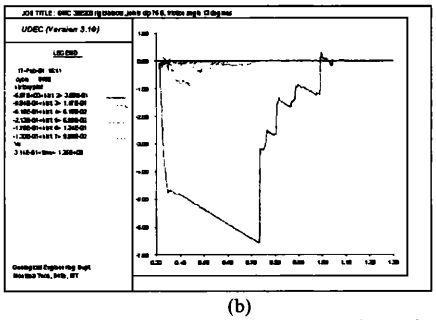

(b)

Figure 10. Plots of vertical component of velocity for blocks extending progressively farther up into the roof of the drift, for configuration with Joint Set #2 dipping 75° S and friction angle a) 12° (deep-seated failure), and b) 13° (roof wedge failure).

5 SIMPLISTIC ANALYTICAL APPROACH

Wedge failures are an extremely common mode of failure in jointed rock, and a number of analytical solutions are available for comparison with the numerical results. Crawford & Bray (1983), Sofianos (1986), and Sofianos et al (1999) have derived equations for predicting the stability of a rock wedge in a tunnel roof, for the cases of both symmetric and asymmetric wedges. The solutions account for the presence of *in situ* stresses in the rock, and shear and normal stiffnesses of the joints.

A much-simplified approach can also be used to provide a rough estimate of wedge stability. Assuming that the two-dimensional wedge-shaped block is symmetric, sliding will not occur if the resultant force on the sides of the wedge is within the "cone of friction" surrounding the normal vectors to both sides (Goodman 1976, 1989). If the weight of the wedge is small compared to the maximum principal stress, which is assumed to be parallel to the roof of the opening, the resultant force may be assumed to have a horizontal orientation. The horizontal resultant will lie inside the friction cone of the normal if the normal is inclined no more than $\phi°$ above horizontal, where ϕ is the friction angle of the surface of contact between the wedge and the rock mass. Since the normal is by definition perpendicular to the side of the wedge, and the wedge is assumed to be symmetric, this condition is satisfied when $\alpha_{1/2}$, half of the apex angle of the wedge, is less than or equal to the friction angle. (Note that $\alpha_{1/2}$ is also equal to 90° minus the dip angle of the side of the wedge, or the complement of the dip angle.) The wedge is predicted to be unstable when $\alpha_{1/2}$ is greater than the friction angle.

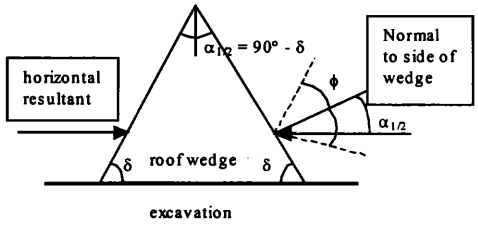

Figure 10. Schematic drawing of roof wedge. δ = dip of joints, ϕ = friction angle of joints, $\alpha_{1/2}$ = half of apex angle.

The predicted results using the rough approach are listed in Table 2. They correspond to the same 11 joint dip angles and 3 friction angles shown in Table 1, and are in complete agreement with the UDEC analyses. Since none of the cases analyzed was symmetric, the half apex angle $\alpha_{1/2}$ is equal to the average of the complement to the 70° dip angle of Joint Set #1 and the complement to the dip angle of Joint Set #2, which varies from 15° to 90°.

Table 2. Roof wedge stability, as a function of the dip angle of Joint Set #2 and friction angle of the joints, as predicted using the rough analytical approach.

Dip of Joint set #2	Half apex angle $\alpha_{1/2}$	Friction angle of joints 15°	30°	45°
15° S	47.5°	unstable	unstable	unstable
30° S	40°	unstable	unstable	stable
45° S	32.5°	unstable	unstable	stable
60° S	25°	unstable	stable	stable
75° S	17.5°	unstable	stable	stable
90°	10°	stable	stable	stable
75° N	2.5°	stable	stable	stable
60° N	5°	stable	stable	stable
45° N	12.5°	stable	stable	stable
30° N	20°	unstable	stable	stable
15° N	27.5°	unstable	stable	stable

In fact, the rough approach can be taken one step further: to identify the friction angle required for stability of the wedge with a given apex angle. Ideally, the wedge would be symmetric, with each half of the apex angle identical to the other, and the friction angle required for stability equal to $\alpha_{1/2}$. A comparison of the friction angle required for stability using calculated using this rough approach and as determined via UDEC analyses is shown in Table 3. These UDEC analyses were performed using the expanded region geometry shown in Figure 8, with fixed boundary conditions. The agreement is quite remarkable, given the rough derivation of the equation, which completely ignores the influence of kinematics, and the asymmetric geometry of the wedges analyzed.

Table 3. Comparison of the friction angle required for stability as a function of the dip angle of Joint Set #2, as calculated using the rough analytical approach and determined with UDEC.

Dip of Joint set #2	Friction angle of joints required for stability Calculated	UDEC results
15° S	47.5°	47° unstable, 48° stable
30° S	40°	40° unstable, 41° stable
45° S	32.5°	32° unstable, 33° stable
60° S	25°	25° unstable, 26° stable
75° S	17.5°	17° unstable, 18° stable
90°	10°	10° unstable, 11° stable
75° N	2.5°	2° unstable, 3° stable
60° N	5°	5° unstable, 6° stable
45° N	12.5°	12° unstable, 13° stable
30° N	20°	20° unstable, 21° stable
15° N	27.5°	28° unstable, 29° stable

It should be noted that the close agreement between the analytical and numerical solutions does not guarantee accuracy with respect to real behavior of the rock. Crawford and Bray (1983) mentioned that their physical model results indicated that the analytical solutions may overestimate the stability of the system, and the discrete element results, particularly since they were produced using rigid blocks, may do the same. Validation using actual field data is a critical component of the process.

6 DISCUSSION

A major theme of this study is to emphasize that it is important to use the right numerical analysis tool for the job. One of the objectives is to provide an example of how continuum models may be used to bracket behavior and identify need for discrete element modeling. However, substantially more joint data are required for adequate representation of the rock mass for discrete element modeling, and the analyses are more computationally intensive. Similarly, parametric discrete element studies can be used to identify ranges of joint spacings (or block sizes) for which discontinuum modeling are appropriate, and which conditions may be adequately modeled with continuum methods.

One primary strength of discrete element modeling is the ability to identify drastic changes in behavior. Because of this, both the details of the model and the range of values used in parametric studies are extremely important, since small changes in parameters can cause large differences in the analysis results.

One of the limitations of this study is that all of the analyses are two-dimensional. A cross-section through a tabular ore body, as modeled here, may be adequately modeled with 2D techniques, but in general, rock stability problems are often three-dimensional in nature.

Additional work to complete the preliminary modeling stage of the project will include parameter sensitivity to further investigate the influence of variability of the material properties, boundary conditions and *in situ* stresses for both continuum and discontinuum analyses, and variation of shear and normal joint stiffness, damping and rounding of block corners for the discontinuum analyses. A complete, comprehensive comparison will be done to quantify the difference in behavior between rigid and deformable blocks. Analysis of the configuration with both drifts using UDEC, and the full suite of DDA analyses will be completed.

More investigation of joint spacing will be done, with both perfect and imperfect joint sets. For perfectly persistent joints, two of the three joint spacing categories produced blocks small enough to behave in a more or less continuous deformation pattern. However, for the case of imperfect joints, these smaller spacings will need to be considered in the discontinuum analyses.

After the preliminary modeling stage is complete, a detailed investigation of the 38E200 drift will be undertaken, using actual field data and comparing predicted and actual performance. Imperfect joint sets will be generated using persistence and bridging data as well as variability of joint dip angles. Support systems will be incorporated as well.

7 CONCLUSIONS

Continuum-based models were used to show that the discontinuities in the rock mass at the Stillwater Mine have the potential to control the behavior of the material. A parametric study was done using discrete element modeling to determine the anticipated types of behavior given a range of possible conditions. While the dip of the joints parallel to the ore zone boundary was held constant at 70°, the dip of the second joint set, friction angle of the joints, and block size were varied. Most cases investigated were either stable due to the high horizontal stress in the rock mass, or were predicted to have the potential for failure of a wedge-shaped roof block whose shape is controlled by the intersecting discontinuities. In general, the stability increased with increasing friction angle, and also with increasing dip angle, since the sides of the wedges produced are more perpendicular to the horizontal orientation of the major principle stress. The results compared very well to behavior predicted using a simplistic analytical approach.

8 ACKNOWLEDGMENTS

This study would not be possible without the cooperation and support of the Stillwater Mining Company, Nye, Montana. Funding is provided by the National Institute for Occupational Safety and Health - Spokane Research Laboratory. Guidance, assistance, and advice provided by NIOSH-SRL personnel, particularly Jeff Whyatt, Mark Larsen, and Jeff Johnson were extremely helpful and greatly appreciated.

9 REFERENCES

Al-Harthi, A & Hencher, S 1992. Physical and numerical modelling of underground excavations in dilational rock masses. In *Proc. ISRM Reg. Conf. on Fractured & Jointed Rock Masses, Lake Tahoe, June 1992:* 608-615. Berkeley: Lawrence Berkeley Laboratory.

Amadei, B 2000. Keynote address (unpublished). *Pacific Rocks, Proc. 4th North American Rock Mechanics Symp., Seattle, 31 July – 3 August 2000.*

Anonymous 2001. Stillwater Mining Company. http://www.stillwatermining.com/ (31 January 2001).

Coulthard, MA, Journet, NC, & Swindells, CF 1992. Integration of stress analysis into mine excavation design. In Tillerson & Wawersik (ed.), *Proc. 33rd US Rock Mechanics Symp., Santa Fe, 3-5 June 1992:* 451-460. Rotterdam: Balkema.

Crawford, AM & Bray, JW 1983. Influence of the *in situ* stress field and joint stiffness on rock wedge stability in underground openings. *Can. Geotech. J.* 20: 276-287.

Czamanske, GK, & Zientek, ML 1985. *The Stillwater Complex, Montana: Geology and Guide, Special Publication 92.* Butte: Montana Bureau of Mines and Geology.

Eve, RA 1996. Modeling of support in deep tabular excavations. In Aubertin et al (ed.), *Rock Mechanics Tools & Techniques, Proc. 2nd North American Rock Mechanics Symp., Montreal, 19-21 June 1996:* 1951-1958. Rotterdam: Balkema.

Goodman, RE 1976. *Methods of Geological Engineering in Discontinuous Rocks.* St. Paul: West Publishing Company.

Goodman, RE 1989. *Introduction to Rock Mechanics, Second Edition.* New York: John Wiley & Sons.

Grenon, M, Hadjigeorgiou J, Harrison, JP, & Banas, R 2000. An investigation of drift stability in moderately jointed rock mass. In Girard et al (ed.), *Pacific Rocks, Proc. 4th North American Rock Mechanics Symp., Seattle, 31 July – 3 August 2000:* 967-973. Rotterdam: Balkema.

Hart, RD, Board, M, Brady, B, O'Hearn, B & Allan, G 1988. Examination of fault-slip induced rockbursting at the Strathcona Mine. In Cundall et al (ed.), *Key Questions in Rock Mechanics, Proc. 29th US Rock Mechanics Symp., Minneapolis, 13-15 June 1988:* 369-379. Rotterdam: Balkema.

Itasca 1998. *FLAC User's Guide (Version 3.4).* Minneapolis: Itasca Consulting Group Inc.

Itasca 2000. *UDEC User's Guide (Version 3.1).* Minneapolis: Itasca Consulting Group Inc.

Johnson, JC, Brady, T, Larson, M, Langston, R, & Kirsten, H 1999. Use of strain-gauged rock bolts to measure rock mass strain during drift development. In Amadei et al (ed.), *Rock Mechanics for Industry, Proc. 37th US Rock Mechanics Symp., Vail, 6-9 June 1999:* 497-502. Rotterdam: Balkema.

Johnson, T, Teller, B, & Trudnowski, J 1997. Crown Pillar Design, Stillwater Mine, Nye, Montana. Montana Tech Geological Engineering Senior Design Project (unpublished), December 1997.

Jung, SJ, Naranjo, PC, Cabrera, F & Lim, HU 1996. Prediction of stope stability at the Las Encinas Mine. In Amadei et al (ed.), *Rock Mechanics for Industry, Proc. 37th US Rock Mechanics Symp., Vail, 6-9 June 1999:* 509-516. Rotterdam: Balkema.

Kirsten, HAD 1996. Report on numerical analysis of the 3100 level shaft and crusher stations, vertical shaft pillar design and 57WB stope. SRK Consulting Engineers Report 208592/2 (unpublished), February 1996.

Kirsten, HAD, and Langston, RB 1998. Report on rock engineering aspects investigated during April visit to mine. SRK Consulting Engineers Report 208592/5 (unpublished), August 1998.

Langston, RB 1997. Report on in-situ stress test. Stillwater Mining Company internal memo (unpublished) 23 September 1997.

Rocscience 1999. *Phase² User's Manual.* Toronto: Rocscience, Inc.

Shen, B and Barton, N 1997. The disturbed zone around tunnels in jointed rock masses. *Int. J. Rock Mech. Min. Sci.* 34(1): 117-125.

Shi, G 1993. *Block System Modeling by Discontinuous Deformation Analysis.* Boston: Computational Mechanics Publications.

Sofianos, AI 1986. Stability of rock wedges in tunnel roofs. *Int. J. Rock Mech. Min. Sci.* 23(2): 119-130.

Sofianos, AI, Nomikos, P, & Tsoutrelis, CE 1999. Stability of symmetric wedge formed in the roof of a circular tunnel: nonhydrostatic natural stress field. *Int. J. Rock Mech. Min. Sci.* 36: 687-691.

Trueman, R, Coulthard, MA & Poulsen, BA 1996. Numerical methods for estimating the stability of unsupported spans for highwall mining. In Aubertin et al (ed.), *Rock Mechanics Tools & Techniques, Proc. 2nd North American Rock Mechanics Symp., Montreal, 19-21 June 1996:* 1985-1992. Rotterdam: Balkema.